UNCLASSIFIED

AD 429925

DEFENSE DOCUMENTATION CENTER

FOR

SCIENTIFIC AND TECHNICAL INFORMATION

CAMERON STATION, ALEXANDRIA, VIRGINIA

UNCLASSIFIED

NOTICE: When government or other drawings, specifications or other data are used for any purpose other than in connection with a definitely related government procurement operation, the U. S. Government thereby incurs no responsibility, nor any obligation whatsoever; and the fact that the Government may have formulated, furnished, or in any way supplied the said drawings, specifications, or other data is not to be regarded by implication or otherwise as in any manner licensing the holder or any other person or corporation, or conveying any rights or permission to manufacture, use or sell any patented invention that may in any way be related thereto.

429925

CATALOGED BY DDC
AS AD No.

THE NOTCH IMPACT BEHAVIOR OF TUNGSTEN

Twenty Second Technical Report

by

R. J. Stokes

C. H. Li

Office of Naval Research Project

Nonr-4076(00) NR-032-451

December 1963

DDC
FEB 24 1964
A 3

H
HONEYWELL

THE NOTCH IMPACT BEHAVIOR OF TUNGSTEN

Twenty Second Technical Report

by

R. J. Stokes

C. H. Li

Office of Naval Research Project

December 1963

Reproduction in Whole or in Part is Permitted
for Any Purpose of the United States Government

Honeywell Research Center

Hopkins, Minnesota

ABSTRACT

This paper compares the fracture behavior of tungsten rods in three conditions, recrystallized, recovered, and wrought. Notched specimens subjected to a 50 in. lb. impact load showed ductile brittle transitions at 700°C, 490°C, and 440°C respectively. The recrystallized material had an equiaxed grain structure and fractured by simple cleavage from a grain boundary source at all temperatures up to 700°C. The wrought and recovered material had an elongated fiberous structure and at low temperatures fractured by cleavage originating from the notch. As the transition temperatures was approached cleavage was preceded by more and more intergranular splitting which deflected the crack front into planes parallel to the tensile axis. The enhanced toughness of wrought and recovered tungsten was attributed both to its inability to initiate cleavage because no grain boundaries were suitably oriented perpendicular to the tensile stress and its inability to maintain cleavage because of intergranular splitting ahead of the crack.

TABLE OF CONTENTS

		Page
ABSTRACT		i
I.	INTRODUCTION	1
II.	EXPERIMENTAL PROCEDURE	2
III.	RESULTS	4
	A. Impact Behavior	4
	B. Electron Fractographic Studies	4
IV.	DISCUSSION	14
REFERENCES		22

LIST OF ILLUSTRATIONS

Figure		Page
1	Microstructures of (a) wrought, (b) recovered, and (c) and (d) recrystallized tungsten. (x250)	3
2	Ductile-brittle transition curves for notched tungsten (A) wrought, (B) recovered, and (C) recrystallized.	5
3	Electron fractograph showing cleavage in recrystallized tungsten, (a) at room temperature (b) at 690°C	6, 7
4	Electron fractograph showing cleavage in wrought tungsten at room temperature	9
5	Wrought tungsten specimen impacted at 460°C. (x6)	9
6	(a) Electron fractograph showing cleavage and intergranular (top) fracture in recovered (1300°C) specimen at 485°C.	11
	(b) Electron fractograph showing intergranular splitting in wrought specimen at 450°C.	12
7	Recovered (1300°C) tungsten specimen impacted at 500°C (x6)	13
8	Source of cleavage fracture in recrystallized tungsten. Impact temperature 700°C. (x250)	15
9	Fracture path in (a) recrystallized and (b) wrought tungsten.	17
10	Ductile-brittle transition curves for notched and unnotched tungsten	21

I. INTRODUCTION

It has been appreciated for a long time in a qualitative manner that the room temperature brittleness of fully recrystallized tungsten may be alleviated by working the material at relatively low temperatures[1]. More recently this difference in mechanical behavior between wrought and recrystallized tungsten has been examined quantitatively by measurement of the tensile properties as a function of temperature. In these experiments brittleness has been expressed in terms of ductility or reduction in cross sectional area upon tensile fracture[2][3][4] or in terms of the bend radius before fracture under bending[5]. This work has shown the existence of a fairly sharp transition from brittle to ductile behavior with an increase in temperature. The ductile-brittle transition temperature for recrystallized material is approximately 200°C higher than for wrought material. An increase in strain rate, small additions of impurity[6], or an increase in grain size[4] shift the respective transition temperatures to higher values but the difference between them remains approximately the same at 200°C.

A number of explanations for this embrittlement by recrystallization have been given. It has been blamed either on the concentration of impurity at the grain boundaries, the increase in grain size or the change in texture which occurs upon recrystallization. The present paper examines the effect of different heat treatments on the notch impact behavior of commercial powder metallurgy tungsten rods. The change in the ductile-brittle transition temperature for this method of loading and the fracture mode has been related to the different microstructures produced by heat treatment.

II. EXPERIMENTAL PROCEDURE

Commercial swaged powder metallurgy tungsten rods 1-3/8" in length and 1/8" in diameter were machined to introduce a sharp V-notch .030" deep. To change the microstructure from that of the as-received wrought material some of the specimens were subjected to an anneal in nitrogen either at 1300°C or 1400°C for 8 hours or at 1600°C or 2000°C for 1/2 hour. The notched rods were then placed in a miniature Charpy type impact machine and struck at their midpoint (opposite the notch) with a hammer designed to deliver 50 in. lbs. of energy. The strain rate at the base of the notch was estimated to be approximately 100 sec^{-1} at the instant of impact. The specimens were heated in situ to the desired impact temperature.

The microstructures produced by the various anneals were studied both by x-ray diffraction and metallographic techniques. Figure 1 reproduces the microstructures observed metallographically following a 10 second electro-etch in a 10 percent KOH solution. Figure 1(a) shows the elongated fibrous grain structure of the as-received material. Following the anneal at 1300°C or 1400°C the grain structure was still elongated as shown in Figure 1(b) but the etch pits delineated dense polygonized dislocation arrays within many of the grains. Occasionally a relatively dislocation free recrystallized grain was found growing into the matrix. The anneals at 1600°C and 2000°C resulted in complete recrystallization and some grain growth. The grains produced at 1600°C were still slightly elongated as shown in Figure 1(c) whereas the anneal at 2000°C produced equiaxed grains. The changes in grain size produced the expected changes in the x-ray back reflection patterns, there was no indication either in the as-received material or the annealed material of any preferred orientation.

(a) As Swaged

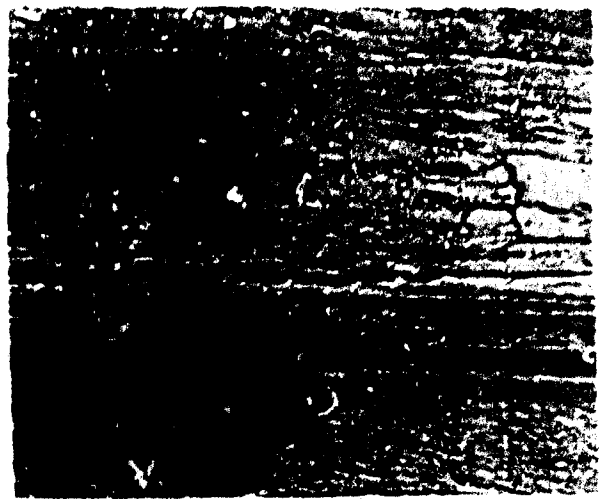

(b) Annealed 8 Hours at 1400°C

(c) Annealed 1/2 Hour at 1600°C

(d) Annealed 1/2 Hour at 2000°C

Figure 1 - MICROSTRUCTURES OF (a) WROUGHT, (b) RECOVERED, AND (c) AND (d) RECRYSTALLIZED TUNGSTEN. (X250)

III. RESULTS

A. IMPACT BEHAVIOR

Figure 2 reproduces the ductile-brittle transition curves measured in the manner described in the previous section. It can be seen that under these testing conditions the as-received wrought tungsten rods showed a ductile-brittle transition between 435°C and 450°C (curve A, Figure 2), whereas the recrystallized material showed a ductile-brittle transition between 690°C and 710°C (curve C, Figure 2), i. e. an increase of 260°C. The polygonized specimens annealed at 1300°C or 1400°C showed a slight increase of 50°C in the ductile-brittle transition temperature to a value between 480°C and 500°C (curve B, Figure 2).

B. ELECTRON FRACTOGRAPHIC STUDIES

The fractured samples were examined both microscopically and with the electron microscope. A two-stage replication technique described elsewhere was used to prepare chromium shadowed carbon replicas[7].

First we shall describe observations on the recrystallized material (curve C, Figure 2). The fracture surfaces over the whole temperature range for which this material was brittle, i. e. up to 700°C, were flat and normal to the rod axis and thus to the tensile direction. Fracture occurred almost exclusively by cleavage with a limited number of intergranular facets. Whereas the cleavage facets at low temperatures were relatively featureless as in Figure 3(a), cleavage facets at temperatures approaching the transition were accompanied by a high density of tear markings and evidence that crack propagation was proceeding discontinuously. Figure 3(b) illustrates the appearance of cleavage in

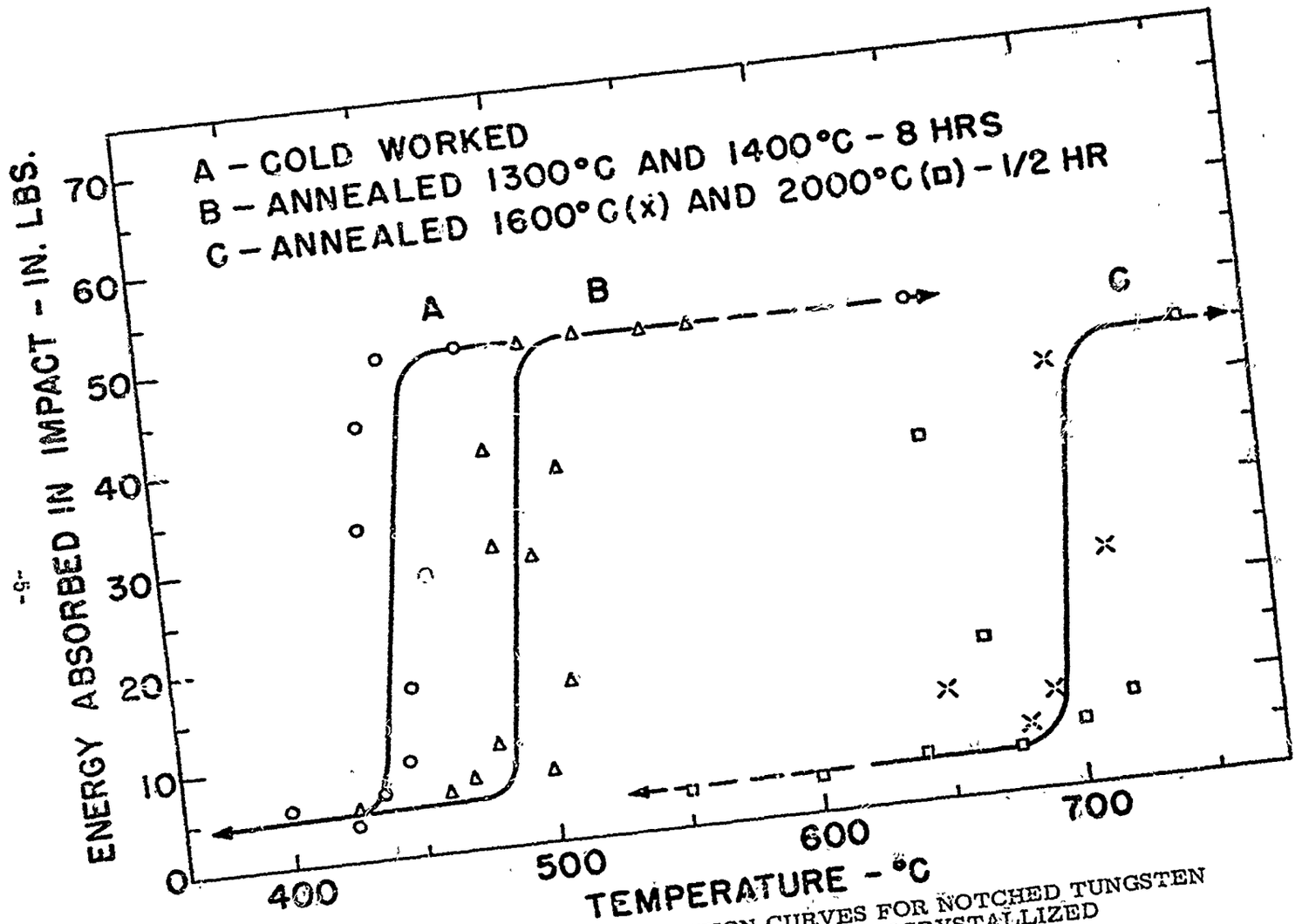

Figure 2 – DUCTILE-BRITTLE TRANSITION CURVES FOR NOTCHED TUNGSTEN (A) WROUGHT, (B) RECOVERED, and (C) RECRYSTALLIZED

Figure 3a - ELECTRON FRACTOGRAPH SHOWING CLEAVAGE IN RECRYSTALLIZED TUNGSTEN AT ROOM TEMPERATURE.

Figure 3b - ELECTRON FRACTOGRAPH SHOWING CLEAVAGE IN RECRYSTALLIZED TUNGSTEN AT 690°C.

recrystallized tungsten at 600°C. The sudden changes in tear line density along a profile corresponding to the crack front in the upper grain of Figure 3(b) indicated discontinuous propagation. In addition it could be seen that fracture in the upper grains was proceeding from left to right and in the lower grains it was proceeding vertically, at the boundary between these two crack fronts there was a narrow zone of plastic tearing. This mode of propagation corresponded to cleavage accompanied by considerable plastic flow at the crack tip, which was to be expected considering the specimen fractured at a temperature only a few degrees below the transition temperature.

The as-received wrought tungsten rods (curve A, Figure 2) and the specimens annealed at 1300°C or 1400°C (curve B, Figure 2) showed a wider spectrum of fracture modes through their respective brittle to ductile transitions. At very low temperatures (i. e. up to 300°C) the wrought specimens fractured predominantly by cleavage with a few isolated regions of intergranular fracture as shown in Figure 4. There were, however, two features which distinguished this low temperature cleavage from that observed on recrystallized material. First, there was a difference in grain size which increased approximately by a factor of 10 in the transverse plane upon recrystallization and second, there was a marked increase in the tear line density. This could have been due to the smaller grain size causing more frequent changes of the fracture plane or due to the higher dislocation density in the wrought material.

As the temperature was raised to 400°C and approached the transition temperature there was an increasing tendency towards intergranular rupture. Since the intergranular surfaces lay parallel to the rod axis this resulted in a rough, stepped fracture surface consisting of islands of cleavage isolated from each other by intergranular cliffs as illustrated in the macrophotograph of Figure 5. Normally these cliffs collapsed in the final replica and could not be seen in the electron microscope but occasionally they became flattened out without rupturing

Figure 4 - ELECTRON FRACTOGRAPH SHOWING CLEAVAGE IN WROUGHT TUNGSTEN AT ROOM TEMPERATURE.

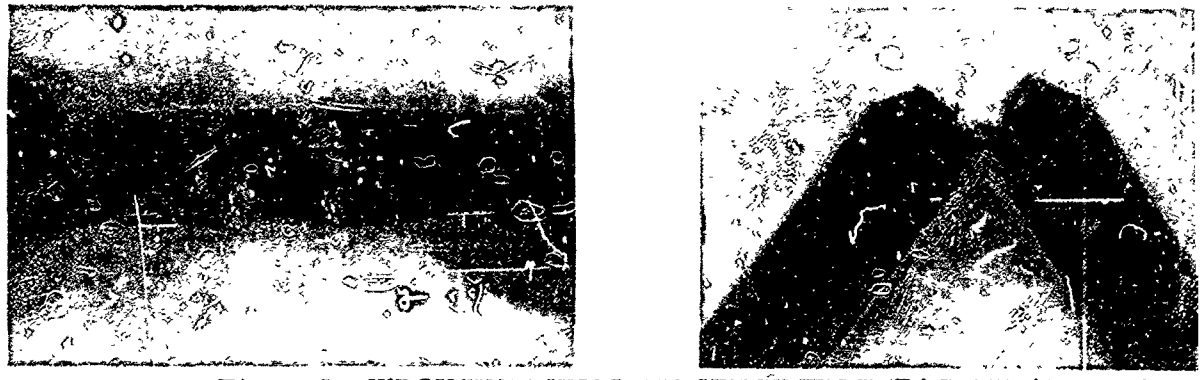

Figure 5 - WROUGHT TUNGSTEN SPECIMEN IMPACTED AT 460°C (X6)

the replica and could then be observed adjacent to and in the same plane as the cleavage facets as shown in Figure 6(a). This particular photograph was taken on a specimen which absorbed 30 in. lbs. in fracturing and was therefore essentially half way up the transition. As Figure 5 also illustrates these specimens generally ended up splitting longitudinally and bending plastically around the hammer. The longitudinal fracture surface was always completely intergranular as illustrated in Figure 6(b). The specimen used for this electron fractograph absorbed 45 in. lbs. and was almost at the top of its brittle to ductile transition.

Those specimens absorbing 45 in. lbs. of energy or more never fractured completely, instead partial splitting occurred by the intergranular mode and the remaining deformation was accompanied by plastic deformation and ductile fracture of the bundles of elongated fibers. An example of this intergranular plus ductile mode is illustrated in the macrophotograph of Figure 7.

In summary, recrystallized specimens fractured simply by cleavage all the way up to the transition temperature above which temperature they bent plastically. Wrought specimens fractured by cleavage at low temperatures, but as the transition temperature was approached there was an increasing tendency for intergranular splitting to occur. At the high energy end of the transition there was no cleavage, instead the specimens split longitudinally over intergranular surfaces and the outer fibers underwent plastic deformation before necking down in bundles to a ductile fracture. Above the transition all of the specimens deformed plastically without fracturing.

Figure 6a - ELECTRON FRACTOGRAPH SHOWING CLEAVAGE AND INTERGRANULAR (TOP) FRACTURE IN RECOVERED (1300°C) SPECIMEN AT 485°C.

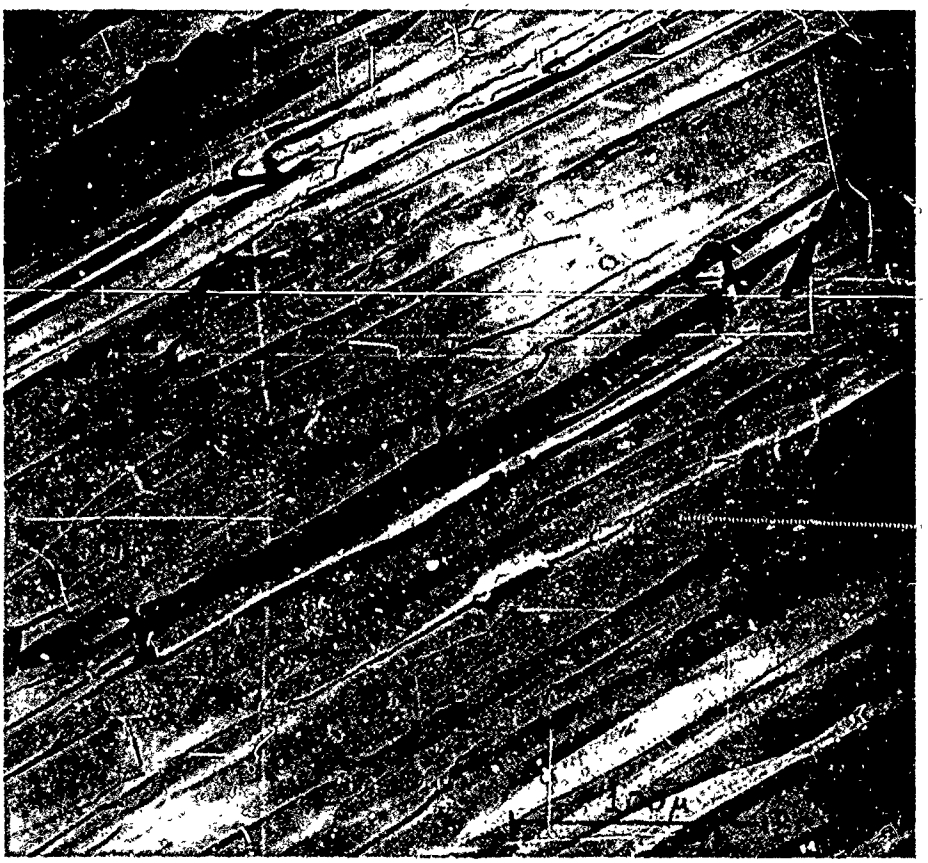

Figure 6b - ELECTRON FRACTOGRAPH SHOWING INTERGRANULAR SPLITTING IN WROUGHT SPECIMEN AT 450°C.

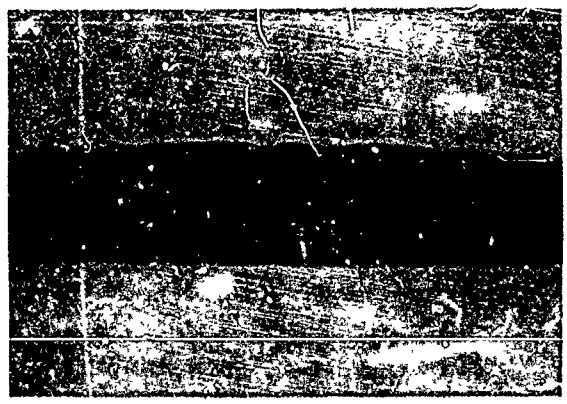

Figure 7 - RECOVERED (13^0°C) TUNGSTEN SPECIMEN IMPACTED AT 500°C. (X6)

IV. DISCUSSION

The most interesting aspect of these tests is the observation that fully recrystallized tungsten fractures predominantly by cleavage at temperatures as high as 700°C and not intergranularly as is normally assumed in the literature. In other words, at all temperatures up to this particular temperature, in equiaxed low dislocation density grains of recrystallized tungsten, it is easier for a cleavage crack to propagate than an intergranular crack. The significant question to be answered therefore is what features of the microstructural changes induced by cold working cause fracture to switch from cleavage to the intergranular mode at low temperatures. The best way to discuss this point is to describe first the apparent sequence of events which occur in the fracture of recrystallized tungsten.

Examination of the fracture source on recrystallized specimens revealed that it was always to be associated with a grain boundary located just below the notch. The cleavage lines on the fracture surface generally focused towards a small intergranular region as illustrated in Figure 8. This intergranular surface was in a plane perpendicular to the tensile direction and fracture propagated away from it over the cleavage planes most nearly perpendicular to the tensile direction, as indicated diagrammatically in Figure 9(a) It may be assumed that the grain boundary provided a microstructural barrier to dislocations participating in the plastic deformation immediately after impact and this together with the development of a triaxial stress state just below the notch caused local intergranular rupture. Once an internal notch had nucleated in this manner it switched into the cleavage plane and any plastic relaxation which may have occurred at the crack tip was insufficient to cause the crack to stall until the temperature approached 700°C.

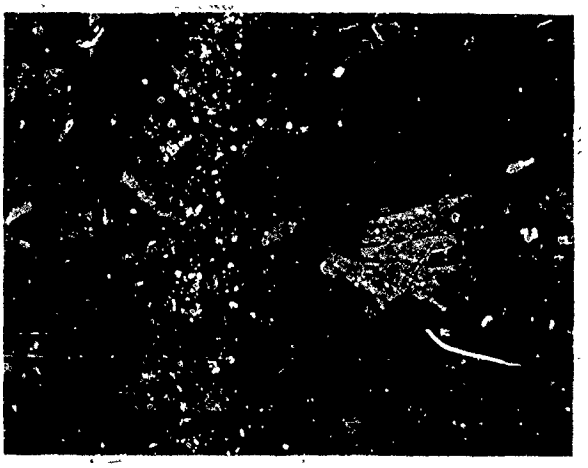

Figure 8 - SOURCE OF CLEAVAGE FRACTURE IN RECRYSTALLIZED TUNGSTEN. IMPACT TEMPERATURE 700°C. (X250)

The critical feature of this fracture process was the generation of an internal flaw in a plane perpendicular to the tensile direction at a very early stage of the low temperature deformation. The fact that it occurred at a grain boundar was not necessarily due to the presence of impurity there but merely a reflection of the role of the grain boundary as a microstructural barrier to dislocations. Brittle fracture in recrystallized b. c. c. metals [8][9][10] and in the pure ionic solids [11] is always found to originate in this way from an intergranular source.

By comparison the sequence of events in the wrought tungsten is considered to be much more complicated. In the first place the pointed shape of the elongate grains in the fibrous structure [12] meant that it was no longer possible for an intergranular crack to nucleate in a plane perpendicular to the tensile direction within the specimen. Instead cleavage had to initiate elsewhere and in these specimens was found to originate at the surface somewhere along the line of the notch, presumably due to the high stress concentration and strain rate there. At low temperatures (i. e. room temperature to 300°C) cleavage nucleated before much bending occurred and was able to propagate across the whole specimen for a simple cleavage fracture normal to the tensile direction. But as the temperature approached 400°C the tungsten became more plastic, there was a delay in the nucleation of cleavage at the notch and the specimen started to bend. As a consequence of this bending and the development of a triaxial stress state beneath the notch, the specimen started to split over longitudinal intergranular surfaces as illustrated diagrammatically in Figure 9(b). Thus when cleavage eventually nucleated at the notch it ran into intergranular fissures and the fracture path was deflected locally into a plane parallel with the tensile direction. The fracture sequence then had to start all over again but this time under less severe loading conditions, because first, the notch effect had been eliminated and second, the strain rate had been lowered due to the reduced specimen

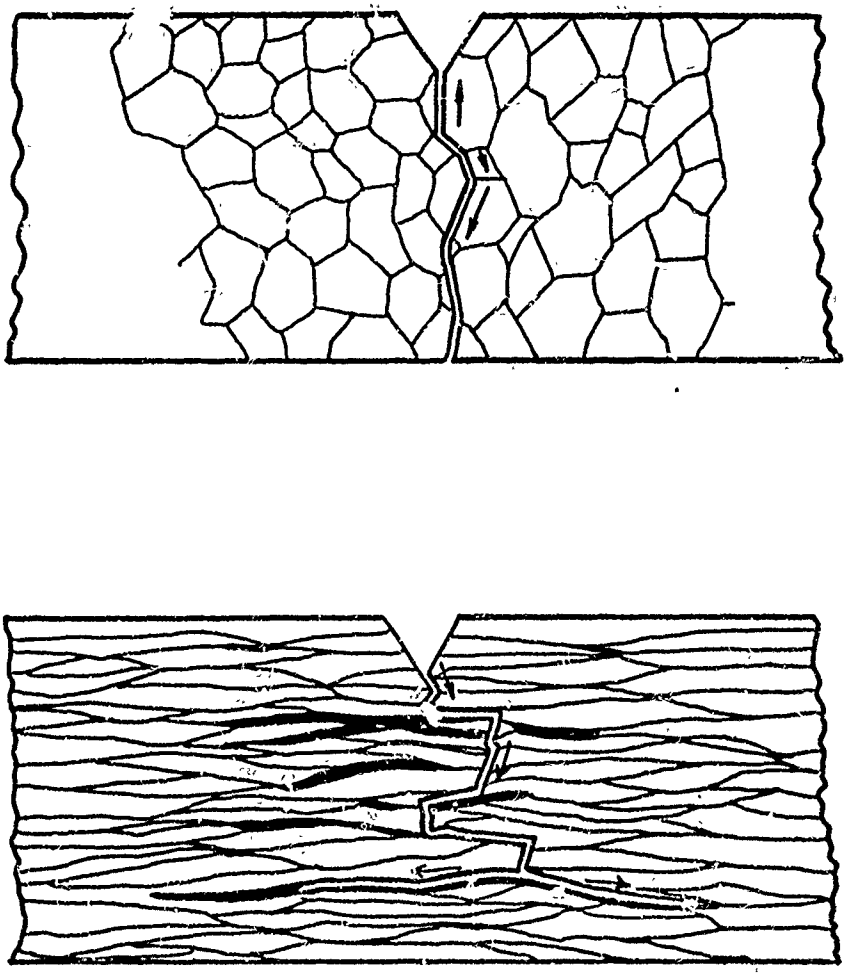

Figure 9 - FRACTURE PATH IN (a) RECRYSTALLIZED AND (b) WROUGHT TUNGSTEN

thickness and loss of momentum by the hammer. After a number of such sequences, switching from cleavage to intergranular and back again (which in fact occurred randomly over the fracture surface), the specimen became thin enough to bend plastically around the hammer, as shown in Figure 5. The change in loading conditions beyond the notch resulted in the situation frequently observed midway through the ductile-brittle transition where cleavage could nucleate from the notch but could not reinitiate subsequently. Instead the columns of elongated grains isolated by intergranular fissures were forced to neck down to a ductile fracture (see Figure 7) and the fracture surfaces consisted of a mixture of cleavage, intergranular and ductile fracture. At the high energy end of the ductile-brittle transition, i. e. around 450°C, cleavage never initiated even at the notch, however, intergranular splitting still occurre and the outer fibers then necked down in the manner shown in Figure 7. Above 450°C the specimens bent without any form of rupture.

The significant feature of the above fracture process is the inability of wrought tungsten to initiate or maintain cleavage in a plane perpendicular to the tensile axis because of the elongated shape of the grains. The question arises as to whether this microstructural change by itself can be solely responsible for the suppression of cleavage and the depression of the ductile-brittle transiti temperature by 260°C. It is our opinion that while the grain shape is the dominant factor the presence of a high density of mobile dislocations and the smaller grain size also make their respective contributions. The important point is that in the absence of suitably oriented grain boundaries cracks have to be generated at the surface or within the grains themselves. Work on tungsten single crystals[13][14] shows that brittle fracture is generally to be associated with twinning, a process which can be suppressed by prior plastic deformation[15]. In this way the high density of mobile dislocations introduced by the low temperature swaging operation may play a role in delaying the initiation of cleavage. Dislocations can also make it more difficult for cleavage to

propagate. When a cleavage crack cuts through a high density of dislocations or low angle boundaries or grain boundaries there is an increase in tear line density and thus in the surface energy to be supplied to the crack face[16]. In addition the availability of a high density of mobile dislocations increases the probability of plastic work accompanying crack propagation. Another factor which could be important in swaged tungsten is the development of the 'spiral nebula' cross sectional grain structure as described by Peck and Thomas[12]. This causes cleavage to follow spiral paths and frequently to reverse its general direction to meet an oncoming crack. The thin strip of material between the two cracks will deform plastically at a moderate temperature (see Figure 3(b) and contribute to the plastic work accompanying crack propagation. These additional features of the microstructure are considered to contribute to the suppression of cleavage in wrought tungsten.

It is not considered that a redistribution of impurity by recrystallization or the change in grain size explain the present results. The redistribution of impurity to grain boundaries would be expected to lead to complete intergranular fracture in the recrystallized material which is clearly not the case and the increase in grain size is not sufficient to cause an increase of 260°C in the ductile-brittle transition temperature upon recrystallization.

On the basis of the above interpretation it is not immediately clear why the recovery anneal at 1300°C and 1400°C should cause an increase of 50°C in the ductile-brittle transition temperature. It could be due to the presence of a few recrystallized grains with intergranular surfaces appropriately oriented perpendicular to the tensile stress or it could be due to the reduction in density and immobilization of dislocations by polygonization. There was no experimental observation capable of resolving these two alternatives.

Finally, it is interesting to consider the role of the notch in the light of the present experiments and their interpretation. For the recrystallized material the notch merely serves to concentrate the stress to rupture the grain boundary

from which cleavage spreads. Eliminating the notch does not remove this intrinsic fracture source and is not expected to have much effect on the ductile-brittle transition behavior of recrystallized tungsten. For wrought material on the other hand the notch not only serves to concentrate the stress but also provides the initial source of cleavage. Eliminating the notch in this case is expected to have a much greater effect on the ductile-brittle transition. Experiments have established that this is in fact the case. As Figure 10 shows, the ductile-brittle transition temperature for unnotched tungsten rods recrystallized at 1610°C for 1/2 hour was measured to be 650°C, a drop of 50°C from the transition temperature for notched recrystallized material. For wrought (as-received) material on the other hand the transition temperature dropped by 140°C (to 300°C) when the notch was eliminated. In addition the wrought material no longer showed the same spectrum of fracture behavior described earlier, once cleavage nucleated at the free surface it propagated virtually without interruption across the specimen. Longitudinal splitting and bending around the hammer illustrated in Figure 5 never occurred with unnotched specimens. This was to be expected since there was no change in loading conditions as fracture propagated through the specimen. The unnotched recrystallized material still fractured by cleavage from an intergranular source located just beneath the surface. In this respect the impact strength of wrought tungsten is more notch sensitive than recrystallized tungsten and therefore more likely to be dependent on surface condition. However, wrought tungsten, notched or unnotched, is always tougher than recrystallized material.

The enhancement of notch toughness through the presence of longitudinal intergranular planes of weakness has now been demonstrated for a variety of materials including ausformed steels[17] and the semibrittle ionic solid silver chloride[18]. All of these solids fracture under impact by the same fracture mode, illustrated in Figure 5, as they approach the transition temperature. It appears that the above observations and interpretation of fracture behavior are common to materials possessing a fiberous texture.

ACKNOWLEDGMENTS

The authors wish to acknowledge the capable assistance of K. H. Olsen and S. Marquardt.

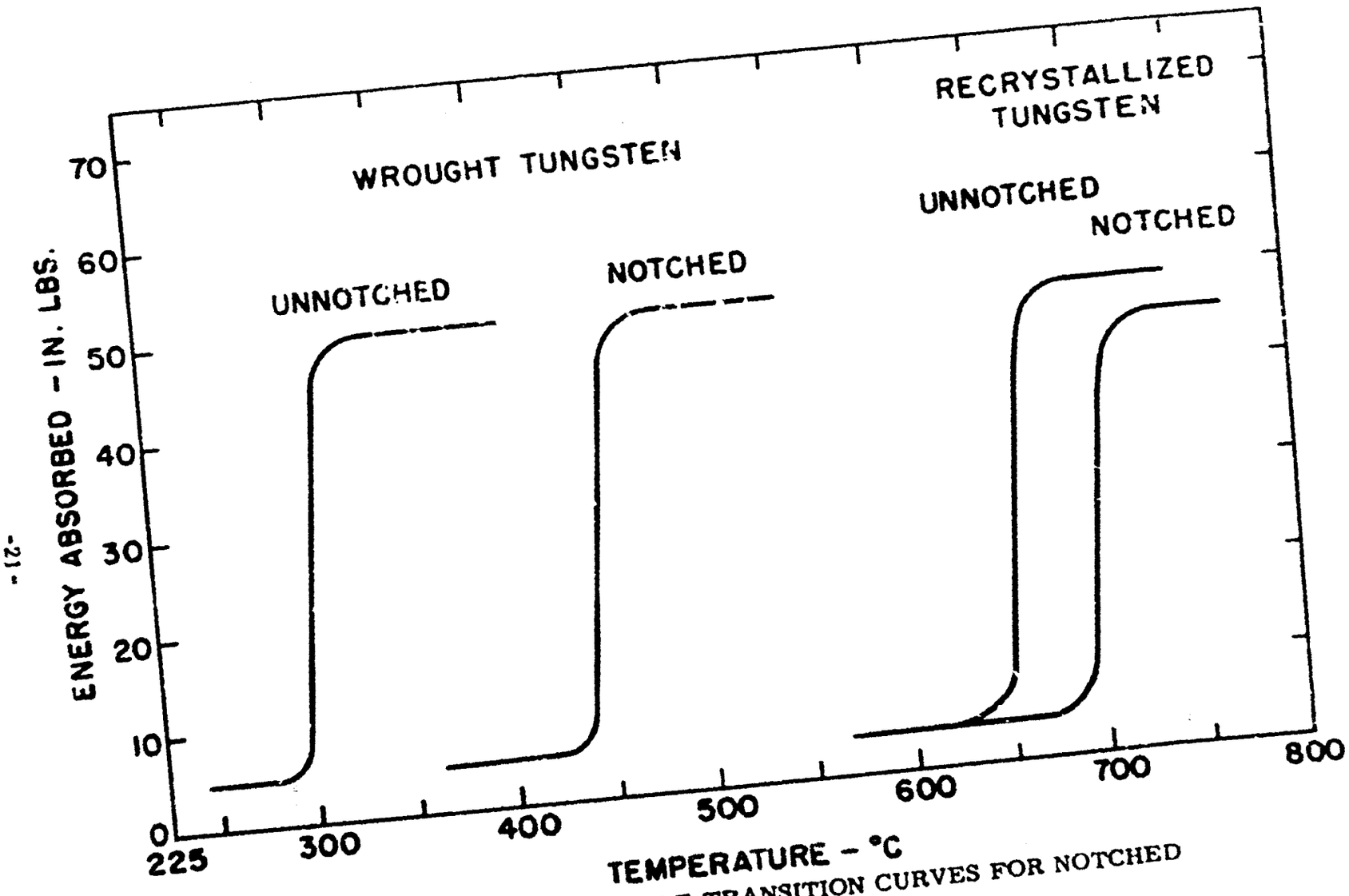

Figure 10 - DUCTILE-BRITTLE TRANSITION CURVES FOR NOTCHED AND UNNOTCHED TUNGSTEN

REFERENCES

1. C. J. Smithells, Tungsten, Chemical Publishing Co., New York, 1953.

2. J. H. Bechtold and P. G. Shewmon, Trans. ASM, vol. 46, p. 397 (1954).

3. J. W. Pugh, Trans. ASTM, vol. 57, p. 906 (1957).

4. R. C. Koo, Trans. Met. Soc. AIME, vol. 227, p. 80 (1963).

5. B. C. Allen, D. J. Maykuth, and R. I. Jaffee, J. Inst. Metals, vol. 90, p. 120 (1961).

6. R. I. Jaffee, B. C. Allen, and D. J. Maykuth, Plansee Proceedings, p. 770 (1961).

7. T. L. Johnston, R. J. Stokes, and C. H. Li, Trans. Met. Soc. AIME, vol. 221, p. 792 (1961). Eleventh Technical Report to O. N. R.

8. J. H. Bechtold, Fracture, John Wiley and Sonc, Inc., New York, p. 628 (1959).

9. R. E. Hook, A. M. Adair, and H. A. Lipsitt, Trans. Met. Soc. AIME, vol. 221, p. 409 (1961).

10. R. E. Hook and A. M. Adair, Trans. Met. Soc. AIME, vol. 227, p. 151 (1963).

11. T. L. Johnston, C. H. Li, and R. J. Stokes, Strengthening Mechanisms in Solids, ASM, Cleveland, Ohio, p. 241 (1962). Tenth Technical Report to O. N. R.

12. J. F. Peck and D. A. Thomas, Trans. Met. Soc. AIME, vol. 221 p. 1240 (1961).

REFERENCES (Cont.)

13. H. W. Schadler, Trans. Met. Soc. AIME, vol. 218, p. 649 (1960).

14. U. E. Wolff, Trans. Met. Soc. AIME, vol. 224, p. 327 (1962).

15. W. D. Biggs, and P. L. Pratt, Acta Met., vol. 6, p. 694 (1958).

16. J. R. Low, Fracture, John Wiley and Sonc, Inc., New York, p. 114 (1959).

17. A. J. McEvily and R. H. Bush, Trans. ASM, vol. 55, p. 654 (1962).

18. T. S. Liu, R. J. Stokes, and C. H. Li, Trans. Met. Soc. AIME, to be published (1964). Twentieth Technical Report to O. N. R.

TECHNICAL REPORT

Distribution List

Nonr-2456(00) NR032-451

Organization	No. of Copies
Chief of Naval Research Department of the Navy Washington 25, D. C. Attention: Code 423	(2)
Commanding Officer Office of Naval Research Branch Office 346 Broadway New York 13, New York	(1)
Commanding Officer Office of Naval Research Branch Office 495 Summer Street Boston 10, Massachusetts	(1)
Commanding Officer Office of Naval Research Branch Office 86 E. Randolph Street Chicago 1, Illinois	(1)
Commanding Officer Office of Naval Research Branch Office 1030 E. Green Street Pasadena 1, California	(1)
Commanding Officer Office of Naval Research Branch Office 1000 Geary Street San Francisco 9, California	(1)
Assistant Naval Attache for Research Office of Naval Research Branch Office, London Navy 100, Box 39 F. P. O., N. Y., N. Y.	(10)
Director U. S. Naval Research Laboratory Washington 25, D. C. Attention: Technical Information Officer, Code 2000	(6)
: Code 2020	(1)
: Code 6200	(1)
: Code 6300	(3)
: Code 6100	(1)
Chief, Bureau of Naval Weapons Department of the Navy Washington 25, D. C. Attention: Code RRMA	(1)
: Code RREN-6	(1)
Commanding Officer U. S. Naval Air Material Center Philadelphia, Pennsylvania Attention: Aeronautical Materials Laboratory	(1)
Picatinny Arsenal Box 31 Dover, N. J. Attention: Lt. Hecht	(1)
Commanding Officer U. S. Naval Ordnance Laboratory White Oaks, Maryland	(1)
Commanding Officer U. S. Naval Proving Ground Dahlgren, Virginia Attention: Laboratory Division	(1)
Chief, Bureau of Ships Department of the Navy Washington 25, D. C. Attention: Code 315	(1)
335	(1)
341	(1)
350	(1)
364	(1)

Organization	No. of Copies
Commanding Officer U. S. Naval Engineering Experiment Station Annapolis, Maryland Attention: Metals Laboratory	(1)
Materials Laboratory New York Naval Shipyard Brooklyn 1, New York Attention: Code 907	(1)
Chief, Bureau of Yards and Docks Department of the Navy Washington 25, D. C. Attention: Research and Standards Division	(1)
Commanding Officer David Taylor Model Basin Washington 7, D. C.	(1)
Post Graduate School U. S. Naval Academy Monterey, California Attention: Dept. of Metallurgy	(1)
Office of Technical Services Department of Commerce Washington 25, D. C.	(1)
Commanding Officer U. S. Naval Ordnance Test Station Inyokern, California	(1)
Armed Services Technical Information Agency (ASTIA) Documents Service Center Arlington Hall Station Arlington, Va.	(5)
Commanding Officer Watertown Arsenal Watertown, Massachusetts Attention: Ordnance Materials Research Office	(1)
: Laboratory Division	(1)

Organization	No. of Copies
Commanding Officer Officer of Ordnance Research Box CM, Duke Station Duke University Durham, North Carolina Attention: Metallurgy Division	(1)
Commander Aeronautical Systems Division Wright-Patterson Air Force Base Dayton, Ohio Attention: Aeronautical Research	
: Lab. (WCRRL)	(1)
: Materials Laboratory (WCRTL)	(1)
: (ASRCEM-1)	(1)
U. S. Air Force ARDC Office of Scientific Research Washington 25, D. C. Attention: Solid State Division (SRQB)	(1)
National Bureau of Standards Washington 25, D. C. Attention: Metallurgy Division	(1)
: Mineral Products Division	(1)
National Aeronautics Space Administration Lewis Flight Propulsion Laboratory Cleveland, Ohio Attention: Materials and Thermodynamics Division	(1)
U. S. Atomic Energy Commission Washington 25, D. C. Attention: Technical Library	(1)
U. S. Atomic Energy Commission Washington 25, D. C. Attention: Metals and Materials Branch	(1)
Division of Research : Eng. Develop. Branch, Division of Reactor Development	(1)

Organization	No. of Copies
Argonne National Laboratory Library Services Dept. Report Section, Bldg 14-Room 14 9700 S. Cass Ave., Argonne, Ill.	(1)
Brookhaven National Laboratory Technical Information Division Upton, Long Island New York Attention: Research Library	(1)
Union Carbide Nuclear Co. Oak Ridge National Laboratory P. O. Box P Oak Ridge, Tennessee Attention: Metallurgy Division	(1)
: Solid State Physics Division	(1)
: Laboratory Records Dept.	(1)
Los Alamos Scientific Laboratory P. O. Box 1663 Los Alamos, New Mexico Attention: Report Librarian	(1)
General Electric Company P. O. Box 100 Richland, Washington Attention: Technical Information Division	(1)
Iowa State College P. O. Box 14A, Station A Ames, Iowa Attention: F. H. Spedding	(1)
Knolls Atomic Power Laboratory P. O. Box 1072 Schenectady, New York Attention: Document Librarian	(1)
U. S. Atomic Energy Commission New York Operations Office 70 Columbus Avenue New York 23, New York Attention: Document Custodian	(1)
Sandia Corporation Sandia Base Albuquerque, New Mexico Attention: Library	(1)
U. S. Atomic Energy Commission Technical Information Service Extensi P. O. Box 62 Oak Ridge, Tennessee Attention: Reference Branch	(1)
University of California Radiation Laboratory Information Division Room 128, Building 50 Berkeley, California Attention: R. K. Wakerling	(1)
Bettis Plant U. S. Atomic Energy Commission Bettis Field P. O. Box 1468 Pittsburgh 30, Pennsylvania Attention: Mrs. Virginia Sternberg, Librarian	(1)
Commanding Officer and Director U. S. Naval Civil Engineering Laborator Port Hueneme, California	(1)
Commanding Officer U. S. Naval Ordnance Underwater Static Newport, Rhode Island	(1)
U. S. Bureau of Mines Washington 25, D. C. Attention: Dr. E. T. Hayes	(1)
Defense Metals Information Center Battelle Memorial Institute 505 King Avenue Columbus, Ohio	(2)
Solid State Devices Branch Evans Signal Laboratory U. S. Army Signal Engineering Laboratories c/o Senior Navy Liaison Officer U. S. Navy Electronic Office Fort Monmouth, New Jersey	(1)

Organization	No. of Copies
U.S. Bureau of Mines P.O. Drawer B Boulder City, Nevada Attention: Electro-Metallurgical Div.	(1)
Commanding General U.S. Army Ordnance Arsenal, Frankford Philadelphia 37, Pennsylvania Attention: Mr. Harold Markus ORDBA-1320, 64-4	(1)
Prof. E. R. Parker Division of Mineral Technology University of California Berkeley 4, California	(1)
D. T. Bedsole, Manager, Technical Library Aerojet-General Corporation Sacramento, California	(1)
Dr. R. A. Lad National Advisory Committee for Aeronautics Lewis Flight Propulsion Laboratory Cleveland, Ohio	(1)
Prof. E. S. Machlin School of Mines Columbia University New York, New York	(1)
Dr. G. T. Murray Materials Research Corp. 47 Buena Vista Avenue Yonkers, New York	(1)
Prof. R. Smoluchowski School of Engineering Princeton University Princeton, New Jersey	(1)
Prof. P. Gibbs Department of Physics University of Utah Salt Lake City, Utah	(1)
Prof. F. H. Norton Department of Metallurgy Massachusetts Institute of Technology Cambridge 39, Massachusetts	(1)
Prof. J. J. Gilman Department of Metallurgy University of Illinois Urbana, Illinois	(1)
Dr. R. G. Breckenridge National Carbon Research Laboratories P.O. Box 6116 Cleveland 1, Ohio	(1)
Dr. J. R. Low General Electric Research Laboratories P. O. Box 1088 Schenectady, New York	(1)
Prof. B. L. Averbach Department of Metallurgy Massachusetts Institute of Technology Cambridge 39, Massachusetts	(1)
Dr. O. L. Anderson Bell Telephone Laboratories Murray Hills, New Jersey	(1)
Prof. W. D. Kingery Department of Metallurgy Massachusetts Institute of Technology Cambridge 39, Massachusetts	(1)
Prof. D. S. Wood Department of Mechanical Engineering California Institute of Technology Pasadena, California	(1)

Organization	No. of Copies
Prof. T. S. Shevlin 303 Roberts Hall University of Washington Seattle 5, Washington	(1)
Dr. B. Post Polytechnic Institute of Brooklyn 99 Livingston Street Brooklyn, New York	(1)
Prof. G. C. Kuczynski University of Notre Dame Notre Dame, Indiana	(1)
Prof. W. H. Robinson Physics Department Carnegie Institute of Technology Pittsburgh, Pennsylvania	(1)
Prof. R. Roy Department of Geophysics Pennsylvania State University University Park, Pennsylvania	(1)
Dr. F. A. Halden Department of Chemistry Stanford Research Institute Menlo Park, California	(1)
Prof. D. H. Whitmore Department of Metallurgy Northwestern University Evanston, Illinois	(1)
Prof. P. J. Bray Department of Physics Brown University Providence, Rhode Island	(1)
Prof. J. O. Brittain Northwestern University Evanston, Illinois	(1)
Prof. W. R. Buessem Department of Ceramic Technology Pennsylvania State University University Park, Pennsylvania	(1)

Organization	No. of Copies
Prof. A. L. Friedberg Department of Ceramic Engineering University of Illinois Urbana, Illinois	(1)
Prof. P. L. Edwards Texas Christian University Fort Worth, Texas	(1)
Prof. I. B. Cutler University of Utah Salt Lake City, Utah	(1)
Dr. B. Phillips Tem-Pres Research, Inc. State College, Pennsylvania	(1)
Prof. J. B. Wagner, Jr. Northwestern University Department of Materials Science Evanston, Illinois	(1)
Prof. W. C. Hahn Department of Metallurgy Montana School of Mines Butte, Montana	(1)
Prof. S. R. Butler Physics Department University of New Hampshire Durham, New Hampshire	(1)
Prof. F. Seitz Department of Physics University of Illinois Urbana, Illinois	(1)
Prof. H. Brooks Dean of Graduate School of Applied Science Harvard University Cambridge, Massachusetts	(1)
Dr. LeRoy R. Furlong Bureau of Mines College Park, Maryland	(1)

Organization	No. of Copies
Prof. W. G. Lawrence New York State College of Ceramics Alfred University Alfred, New York	(1)
Prof. A. von Hippel Laboratory for Insulation Research Massachusetts Institute of Technology Cambridge 39, Massachusetts	(1)
H. R. Peiffer RIAS Inc. 7212 Bellona Avenue Baltimore 12, Maryland	(1)
Prof. J. Gurland Division of Engineering Brown University Providence, Rhode Island	(1)
Dr. J. T. Ransom Engineering Research Laboratory Experiment Station E. I. duPont and Co., Inc. Wilmington, Delaware	(1)
Dr. F. J. P. Clarke Metallurgy Division A. E. R. E. Harwell, Berkshire, England	(1)
Dr. R. Chang Atomics International P. O. Box 309 Canoga Park, California	(1)
Dr. I. Cadoff New York University University Heights New York, New York	(1)
Prof. F. V. Lenel Department of Metallurgical Engineering Rensselaer Polytechnic Institute Troy, New York	(1)
Prof. J. A. Pask Dept. of Mineral Technology University of California Berkeley 4, California	(1)
Prof. D. Turnbull Div. of Engineering and Applied Physics Pierce Hall Harvard University Cambridge 38, Massachusetts	(1)
Dr. J. B. Wachtman, Jr. National Bureau of Standards Division 9.6 Washington 25, D. C.	(1)
Dr. J. J. Duga Battelle Memorial Institute 505 King Avenue Columbus 1, Ohio	(1)
Dr. W. P. Shulof Dept. 32-26 AC Spark Plug Division Flint, Michigan	(1)
Dr. R. M. Spriggs Metals and Ceramics Research AVCO Corp. 201 Lowell Street Wilmington, Massachusetts	(1)